

NUMERICAL SIMULATION OF FILM COOLING IN HYPERSONIC FLOWS

Xiaobo Yang*, K. J. Badcock†, B. E. Richards‡ and G. N. Barakos§

*Department of Aerospace Engineering
University of Glasgow
Glasgow, G12 8QQ
Scotland, UK*

Abstract

In this paper, a numerical study of film cooling in both laminar and turbulent hypersonic flows has been performed. The aim of this computational work was to investigate the mechanism and effectiveness of film cooling in hypersonic flows. The coolant fluid was found to affect the primary boundary layer in two ways: 1) a separate boundary layer established by the coolant fluid itself, 2) a mixing layer between the primary and coolant flow streams. According to the analysis of the film cooling effectiveness, it has been revealed that under the same primary flow conditions the flow field of film cooling could be recognized as two separate regions. These two regions are divided by the point of the cooling length x_A . For laminar flow, film cooling effectiveness was observed to obey a second-order curve in the log-log coordinates against $\log_{10}\eta = f(\log_{10}\frac{x}{hm})^2$. For turbulent flow, a linear relation was found suitable to describe the relation between $\log_{10}\eta$ and $\log_{10}\frac{x}{hm}$.

Nomenclature

h	step height (slot height plus slip height)
l	lip height
L	length of flat plate downstream of the slot exit
\dot{m}	the ratio of coolant mass flux per unit area to primary stream mass flux per unit area, $\dot{m} = \rho_c u_c / \rho_\infty u_\infty$
M	Mach number
p	pressure
\dot{q}	heat transfer rate
Re	Reynolds number
s	slot height
T	temperature
u	velocity
x	distance downstream of the slot exit
x_A	cooling length
y	a group of parameters, $y = \log_{10}\frac{x}{hm}$
y^+	dimensionless wall distance
η	film cooling effectiveness, $\eta = 1 - \dot{q}_c / \dot{q}_0$
μ	laminar molecular viscosity
μ_t	turbulent eddy viscosity
ρ	density

Subscripts

0	stagnation/reference
ad	adiabatic
c	coolant flow
w	wall
∞	freestream

Introduction

By introducing a coolant fluid, film cooling is used to provide heat protection for wall surfaces under high thermal load, such as turbine blades and combustion chamber and inlet walls of scramjets. Olsen *et al.*¹ and Garg² gave two examples of the application of film cooling in their papers. Film cooling is applied in a scramjet engine combustor wall¹ with some hydrogen fuel injected parallel to the wall through small supersonic slots to provide a lower energy buffer layer between the engine core flow and the structure. The other example given by Garg² is an ACE turbine. Modern gas turbine engines are designed to operate at turbine inlet temperatures of about 2000 K, which value is far beyond the allowable metal temperature. The turbine blades need to be cooled under these conditions in order to increase their lifetime. So an efficient cooling system needs be provided. Discrete jet film cooling is applied in this turbine blade with 93 holes on each rotor blade.

Many experimental results have been published³⁻⁹ for the film cooling problem. Although primary and coolant flow stream velocities are often quite different,

*Postgraduate Student

†Senior Lecturer

‡Mechan Professor, AFAIAA

§Lecturer

Copyright © 2003 by the American Institute of Aeronautics and Astronautics, Inc. All rights reserved.

the flow is distinguished by the primary flow stream velocity. Film cooling effectiveness was found to be influenced by many parameters. Researchers offered different empirical equations to predict the effectiveness of film cooling. But usually such equations are only valid in a narrow scope related to similar conditions used in the experiment. Different parameters were studied such as slot height, lip thickness, flow density and velocity ratios between the primary and the coolant flow and a coolant gas different from the primary one. Besides the experimental study of film cooling in subsonic and supersonic areas, a lot of experimental work in hypersonic film cooling^{1,10-16} has been done in the past forty years. But since the film cooling problem is very complex, as mentioned above, it has been found that it is really difficult to achieve a universal equation to predict the film cooling effectiveness according to the experimental results. Thus there is importance in performing a numerical study of film cooling to contribute to added understanding of the film cooling effectiveness. Usually the slot height used is very small (several millimeters), therefore, it is made difficult to measure detailed information of the conditions of the flow in the near slot area by experiment. Computational Fluid Dynamics (CFD) provides the opportunity to investigate the full developing flow field in detail including within the near slot region.

Although some numerical studies^{2,17-21} have been performed to investigate the film cooling problem, they are mainly focused on subsonic and supersonic flows. Nowadays, there is a resurgence of interest in hypersonic flight and rockets, so it is important to execute a numerical study of film cooling in hypersonic flows. The purpose of this study is to simulate film cooling in both hypersonic laminar and turbulent flows choosing the cases used in the experimental work of Richards.¹⁰ Different gases were used in these experiments, but only air was considered in this study.

Numerical Methods

The PMB2D code²² developed at the University of Glasgow was used to perform this CFD study in both laminar and turbulent hypersonic film cooling problems. The Navier-Stokes equations are discretized in space using a cell-centered finite volume approach. The convective terms are discretized using either the Osher or Roe scheme. All calculations in this study were obtained using the Roe scheme. The Harten entropy fix²³ was introduced in the Roe scheme in order to avoid the occurrence of non-physical expansion shocks. MUSCL variable interpolation is employed to achieve 2nd order spatial accuracy. The diffusive terms are discretized by central differencing. A time-marching scheme is performed to get a steady solution. Further details of the numerical methods used in PMB2D was reported by Badcock *et al.*²² and Can-

tariti *et al.*²⁴

Besides the standard Wilcox $k - \omega$ turbulence model²⁵ in the PMB2D code, Menter's baseline and SST models²⁶ have been tested during the hypersonic turbulent film cooling study. Although Menter's models were observed to work well in transonic and hypersonic flat plate flows,²⁷ Wilcox's $k - \omega$ model with dilatation-dissipation correction (Zeman's free shear layer model²⁸) gave the best heat prediction in the turbulent film cooling case.

The computational domain is shown in Fig. 1. In this paper, the lip thickness is 0.0508 mm and the slot height is 1.6002 mm (these values were converted from the unit used by Richards,¹⁰ inches, four digitals are kept here after the decimal point for easy treatment when generating the meshes). Different slot heights were also studied by Yang²⁷ but will not be discussed in this paper. For laminar cases, the inclusion of the coolant inlet duct was observed to provide improved heat transfer rate prediction rather than a simple profile set up at the slot exit directly.²⁷ For turbulent cases, block 1 in Fig. 1 was extended upstream to 152.40 mm according to the experiment.

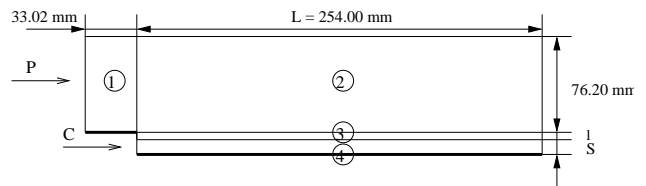


Fig. 1 Computational domain of the film cooling problem

Freestream conditions were set at the leading edge and at the top of the computational domain. For turbulent flow, a turbulent boundary layer profile was set up at the leading edge. A simple first-order extrapolation from the interior was applied at the outlet. For laminar flow, a uniform boundary layer was set up at the extended inlet of the coolant duct. For turbulent flow, a uniform boundary layer was set up at the slot exit and the coolant flow was supposed to be choked which was observed in the laminar cases.²⁷ The primary flow conditions considered in this study are listed in Table 1. In the experiments, a conical nozzle was used for all laminar cases while a contoured nozzle was used for all turbulent cases. Therefore recalculated flow conditions for laminar cases was listed in Table 1.²⁷

Table 1 Primary flow conditions

Flow type	M_∞	Re/m	p_∞ (Pa)	T_∞ (K)
Laminar	9.90	6.46×10^6	476.00	62.62
Turbulent	8.20	2.21×10^7	957.00	53.64

Five coolant injection rates were calculated in both

the laminar and turbulent film cooling simulations. For the laminar flow, the coolant injection rate varied from 2.95×10^{-4} to $7.33 \times 10^{-4} \text{ kg/s}$ and for the turbulent flow from 5.07×10^{-4} to $30.69 \times 10^{-4} \text{ kg/s}$. Table 2 lists both laminar (LFC Case 1-5) and turbulent (TFC Case 1-5) coolant flow conditions used in this study. For laminar flow, the flow conditions are at the extended inlet²⁷ while for turbulent flow at the slot exit as shown in Fig. 1.

Table 2 Coolant flow conditions

Case	M_c	ρ_c (kg/m^3)	p_c (Pa)	T_c (K)
LFC Case 1	0.1	1.07×10^{-2}	885.50	289.42
LFC Case 2	0.1	1.47×10^{-2}	1226.08	289.42
LFC Case 3	0.1	1.83×10^{-2}	1521.25	289.42
LFC Case 4	0.1	2.21×10^{-2}	1839.12	289.42
LFC Case 5	0.1	2.65×10^{-2}	2202.40	289.42
TFC Case 1	1.0	1.17×10^{-2}	809.34	241.67
TFC Case 2	1.0	1.95×10^{-2}	1352.93	241.67
TFC Case 3	1.0	3.27×10^{-2}	2270.98	241.67
TFC Case 4	1.0	4.84×10^{-2}	3358.16	241.67
TFC Case 5	1.0	7.07×10^{-2}	4904.36	241.67

It was found that the farfield freestream temperature T_∞ is very low compared with the wall temperature T_w , the temperature gradient is thus high in the area very close to the wall surface. It was found that an iteration procedure using incremental values of T_∞ was necessary to approach the required value T_w/T_∞ (about 5.0). A typical temperature iteration for laminar cases is $T_w/T_\infty = 1.5, 2.5, 4.0, 4.62$. In each iteration, the flow field of the last step was used as the initial flow field for the following case.

As well as the isothermal wall condition applied in the experiment, all physical surfaces are modelled as no-slip (viscous flow) isothermal wall surfaces. Zero pressure gradient is used on these wall surfaces. An adiabatic wall was also investigated in LFC Case 3 since it is more widely used in experimental studies and practical engineering applications. Also the benefit of using such an adiabatic wall boundary condition can save a lot of computing cost since there does not exist a strong temperature gradient near the wall.

A grid resolution study has been executed on both laminar and turbulent calculations. The grid in the near slot region is shown in Fig. 2. For both coarse and fine meshes, the grid was made fine enough to make the dimensionless wall distance $y^+ < 0.1$ for the first grid point above the wall. In the area near the wall and the slot exit, dense meshes were generated. A typical mesh for the turbulent flow contains 27,587 grid points ($92 \times 75, 151 \times 75, 151 \times 9, 151 \times 53$ in blocks 1-4 respectively).

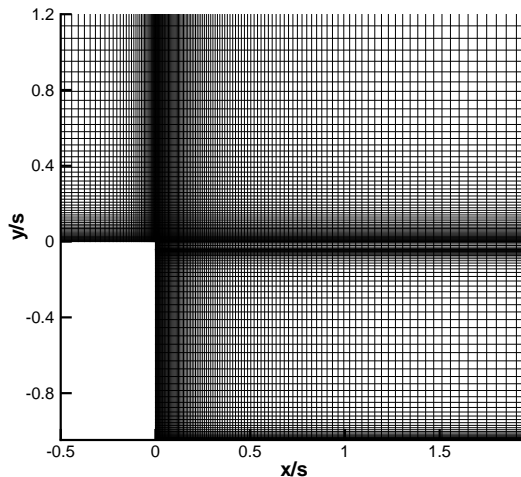


Fig. 2 Grid topology in the near slot area

Results and Discussion

Heat transfer rate comparison

Heat transfer rates for laminar and turbulent cases are compared with the experimental data in Fig. 3 and 4 respectively.

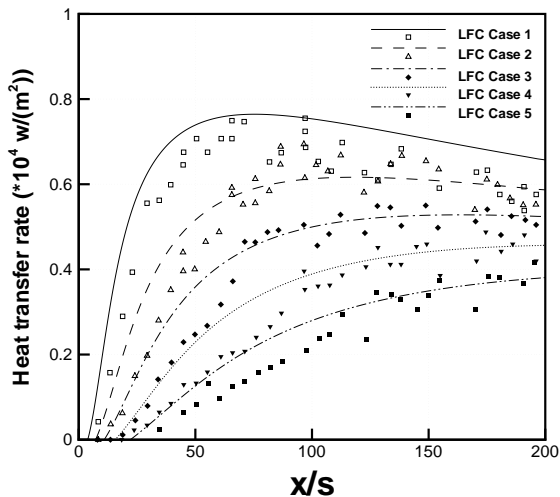


Fig. 3 Heat transfer rate comparison for laminar flows

The agreement of the heat transfer rate for laminar flow is relatively good while for turbulent flow it is more difficult to predict the heat transfer rate the same level as the laminar flow. Here the key issue is the turbulence model. The inaccurate inlet geometry could play an important role which was observed by Yang.²⁷ Also in the experiments, it was found difficult to obtain fully two dimensional injection of the coolant.

In these five TFC Cases, the experimental cooling length changes only by a small amount in the experi-

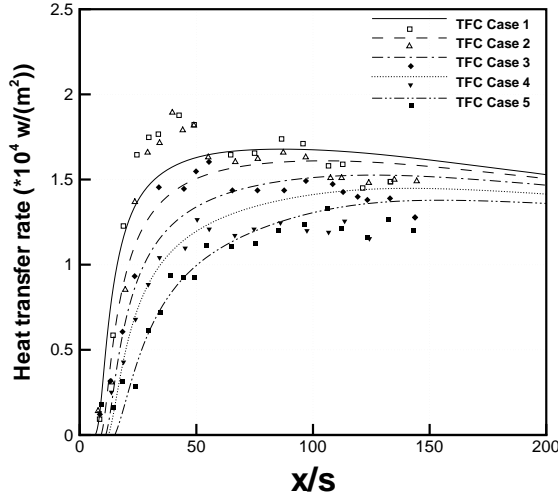


Fig. 4 Heat transfer rate comparison for turbulent flows

ment. In the computational results, the cooling length has a more definite increase with increase in coolant injection rate because more momentum and energy were injected into the primary flow stream through the given profile applied at the slot position. Although the turbulent eddy viscosity μ_t is set to $4,000 \mu_\infty$ at the coolant inlet, it will peter out so that a laminar region occurs, which will lead to an increase of the cooling length. The coolant flow influences the primary flow even far downstream of the slot in all the turbulent cases, but less in the computational study than the experiments.

Film cooling mechanism analysis

The static temperature contour of a typical laminar film cooling case (LFC Case 3 in Table 2) is shown in Fig. 5. In Fig. 6 an amplified temperature boundary layer in the near slot region is depicted. The higher temperature layer of the primary flow stream is clearly observed to be moved away from the surface downstream of the slot position. Then the temperature becomes increasingly lower. From about 40 s downstream of the slot (Fig. 5), a new higher temperature layer develops and moves towards the wall surface. This shows similar behavior as the velocity profiles with distance downstream of the slot exit.

According to the above temperature contours, the main contribution to heat protection by film cooling was observed to be the separate coolant boundary layer keeping the primary boundary layer away from the surface. Further downstream the coolant fluid mixes with the primary fluid, leading to the development of a new boundary layer. Thus, it can be concluded that the development of the primary boundary layer is affected by the injection. For both laminar and turbulent film cooling, it will be shown later that the effectiveness can be described by two equations

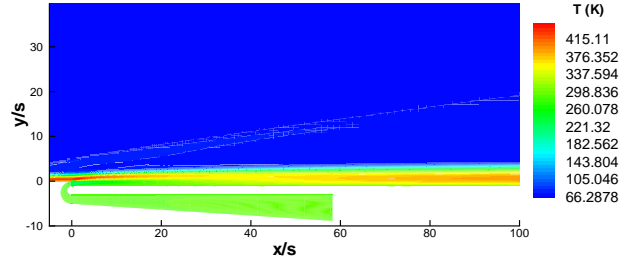


Fig. 5 Static temperature contour of a typical laminar film cooling case

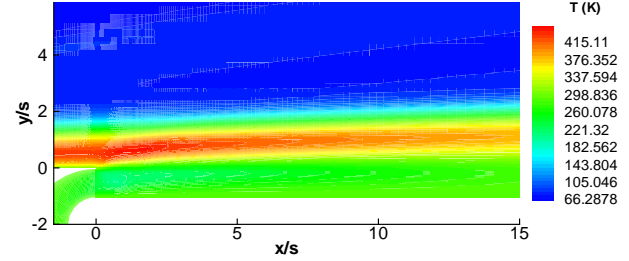


Fig. 6 Amplified static temperature contour in the near slot region

within and downstream of the cooling length.

Isothermal and adiabatic wall

The calculation of LFC Case 3 was repeated assuming an adiabatic wall, instead of an isothermal wall for hypersonic laminar film cooling using otherwise the same flow and coolant conditions. Benefits of using the adiabatic wall instead of the isothermal wall were found in the reduction of the computational cost because there is no temperature gradient between the fluid and the wall surface.

The film cooling effectiveness for an adiabatic wall can be defined in Eqn. (1).

$$\eta_{ad} = \frac{T_{ad,w} - T_0}{T_c - T_0} \quad (1)$$

$T_{ad,w}$, T_c and T_∞ in Eqn. (1) represent the adiabatic wall, coolant and freestream flow temperatures, respectively. This definition has been more widely used in the literature, mainly because continuous/long duration wind tunnels have been used to generate data, when adiabatic conditions have been achieved. Also designers tend to use information about effectiveness in this form. This exercise is thus useful to determine how similar results can be achieved from these two definitions.

For the isothermal wall condition, the film cooling effectiveness is defined by

$$\eta = 1 - \frac{\dot{q}_c}{\dot{q}_0}, \quad (2)$$

where \dot{q}_c and \dot{q}_0 are the heat transfer rate coefficients with and without film cooling. A flat plate case was

used here to provide the reference datum as the without film cooling case.

The film cooling effectiveness from both calculations is compared in Fig. 7. The agreement between these two different wall boundary conditions is very good in the near slot region with the isothermal wall case giving slightly higher film cooling effectiveness. In the area far from the slot, however the adiabatic wall eventually gives somewhat higher effectiveness. In this laminar case, the conical nozzle used in the experiment was not simulated. Although the heat transfer rate was found not to be sensitive to the geometry configuration,²⁷ discrepancy in the region far from the slot position should be larger than the area near the slot. Thus film cooling effectiveness calculated by the heat transfer rate is more meaningful in the near slot area. Therefore, accepting small errors the adiabatic wall assumption could be used instead of the isothermal wall with the benefit of reduction of the computational cost.

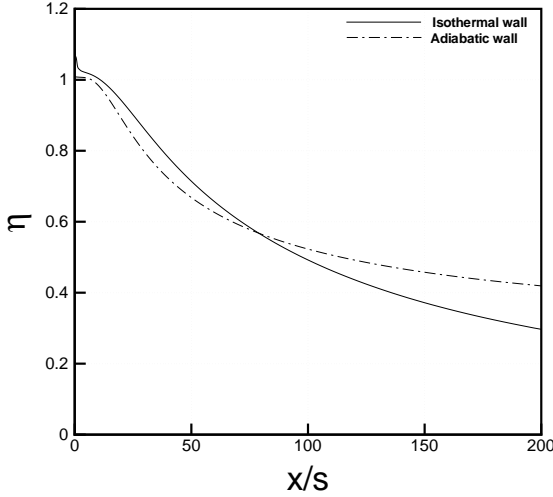


Fig. 7 Laminar film cooling effectiveness using different wall conditions

It is also noted that the wall temperature in the experiments slightly change even though the duration of each experiment was very short (about 40 *ms*), but this is thought not to be significant in the assessment of film cooling effectiveness. In practice it is noted that during a flight of a hypersonic vehicle the wall conditions are likely to be somewhere in between an isothermal and an adiabatic wall case.

Analysis of the results

Curve fitting is commonly used as a means of analysis in nearly all the experimental and numerical film cooling studies.^{7, 13, 14, 16, 19, 29-32} According to experimental data, the film cooling efficiency η is usually described in these works as a function of the nondimensional distance from the slot exit x/h (h may be the slot height s or the step height $s + l$, l is the

lip thickness) and the ratio of coolant mass flux per unit area to primary stream mass flux per unit area \dot{m} ($\dot{m} = \rho_c u_c / \rho_\infty u_\infty$), i.e., $\eta = f\left(\frac{x}{h\dot{m}}\right)$. Based on previous experimental results, this function was usually expressed in log-log coordinates, $\log_{10}\eta = f\left(\log_{10}\frac{x}{h\dot{m}}\right)$. Suppose that $y = \log_{10}\frac{x}{h\dot{m}}$, the function can normally be divided into three segments: 1) $y \leq y_A$, from the slot exit to the cooling length point, the wall surface is fully cooled, i.e., $\eta \geq 1$, 2) $y_A < y < y_C$, is the region when mixing between the primary and the cooling flow streams occurs, 3) $y \geq y_C$, the coolant and primary flow streams tend to be fully merged when a power law was found suitable to describe the relationship for the region.

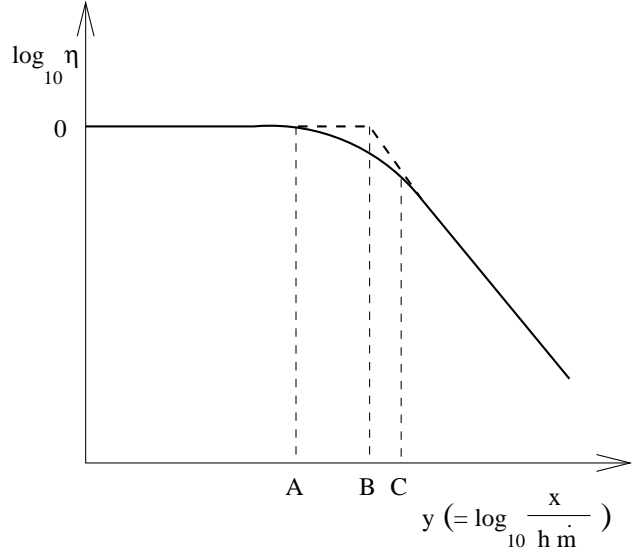


Fig. 8 Film cooling effectiveness

In the current study, for both the laminar and turbulent flows, only two separate regions were recognized: 1) $y \leq y_A$, inside the cooling length (which is an average cooling length for all cases), 2) $y > y_A$, outside the cooling length. For the laminar cases, after the cooling length a power curve was determined by curve fitting the numerical results to describe the effectiveness of the later region as illustrated in Fig. 9. However for the turbulent cases, a straight line was similarly determined to represent the effectiveness in a log-log representation.

Thus for both laminar and turbulent flows, a two-equation model has been established for predicting film cooling effectiveness against parameter $x/(h\dot{m})$. The second relation was as simple as a linear curve for turbulent flows, while a second-order polynomial curve was used to fit the laminar film cooling effectiveness in log-log coordinates.

Laminar flow :

$$\log_{10}\eta = \begin{cases} 0 & y \leq y_A \\ -0.45y^2 + 1.79y - 1.80 & y > y_A \end{cases} \quad (3)$$

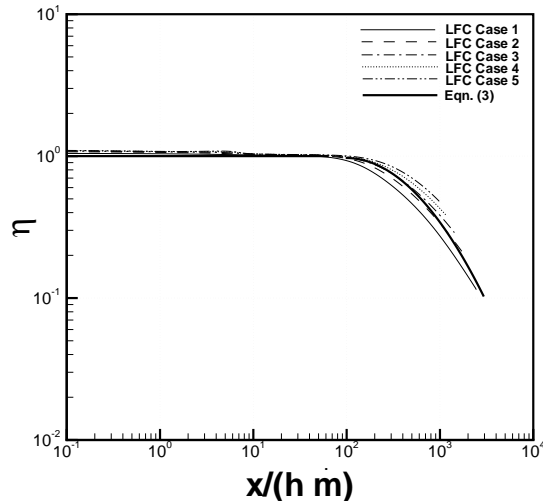


Fig. 9 Film cooling effectivenesses of laminar cases comparing with curve fitting result

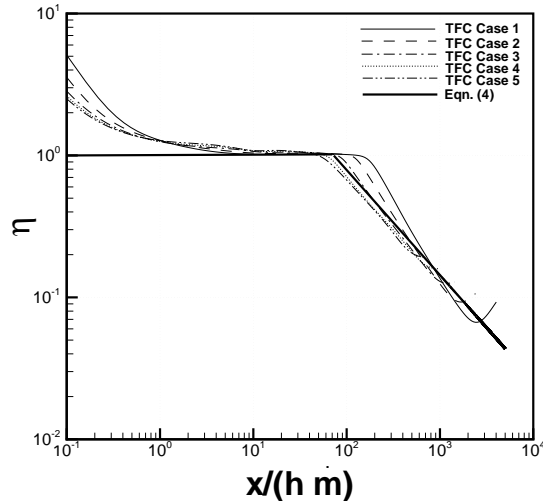


Fig. 10 Film cooling effectivenesses of turbulent cases comparing with curve fitting result

Turbulent flow :

$$\log_{10}\eta = \begin{cases} 0 & y \leq y_A \\ -0.74y + 1.38 & y > y_A \end{cases} \quad (4)$$

In the above two equations, y equals $\log_{10}\frac{x}{hm}$. The turbulent film cooling effectiveness is defined directly by Eqn. (4). The quantity y_A here is defined as an average value of $\log_{10}\frac{x_A}{hm}$ for LFC Cases 1-5 or TFC Cases 1-5 for laminar and turbulent flows accordingly and is given as

$$y_A = \frac{1}{n} \sum_{i=1}^n \left(\log_{10} \frac{x_A}{h \dot{m}} \right). \quad (5)$$

The quantity x_A in Eqn. (5) is the cooling length within which the wall surface is fully heat protected by the coolant fluid. A curve fitting procedure has also been carried out to estimate the cooling length x_A .

$$x_A/h = \begin{cases} 405.83 \dot{m}^{1.86} & \text{laminar flow} \\ 24.36 \dot{m}^{0.44} & \text{turbulent flow} \end{cases} \quad (6)$$

In this study, due to the constant step height, a simple treatment of the step height was applied in Eqn. (6). This was observed²⁷ to be not precise enough for predicting the cooling length when the step height is varied.

Conclusions

A numerical study of film cooling in both laminar and turbulent hypersonic flows has been performed. Film cooling in both laminar and turbulent hypersonic flows can be divided into two regions – within and downstream of the cooling length. By curve fitting the results in appropriate parameters, this leads to a simple two-equation model to predict the film cooling effectiveness. For laminar flow, film cooling effectiveness was found to obey a second-order equation of the form $\log_{10}\eta = f(\log_{10}\frac{x}{hm})^2$ while for turbulent flow, a linear relation was found suitable to describe the relation between $\log_{10}\eta$ and $\log_{10}\frac{x}{hm}$ which leads to a power law in these coordinates.

Using adiabatic wall conditions as an assumption in the calculation instead of isothermal wall conditions, it is shown to give reasonable results for film cooling effectiveness whilst reducing computational cost. This observation is useful in future three-dimensional numerical study for hypersonic film cooling.

References

- ¹Olsen, G., Nowak, R., Holden, M., and Baker, N., "Experimental results for film cooling in 2-D supersonic flow including coolant delivery pressure, geometry, and incident shock effects," *AIAA Paper 90-0605*, 1990.
- ²Garg, V., "Heat transfer on a film-cooled rotating blade using different turbulence models," *International Journal of Heat and Mass Transfer*, Vol. 42, 1999, pp. 789–802.
- ³Burns, W. and Stollery, J., "The influence of foreign gas injection and slot geometry on film cooling effectiveness," *International Journal of Heat and Mass Transfer*, Vol. 12, 1969, pp. 935–951.
- ⁴Jr., R. C., Ng, W., Walker, D., and Schetz, J., "Large-scale structure in a supersonic slot-injected flowfield," *AIAA Journal*, Vol. 28, No. 6, 1990, pp. 1045–1051.
- ⁵Bass, R., Hardin, L., Rodgers, R., and Ernst, R., "Supersonic film cooling," *AIAA Paper 90-5239*, 1990.
- ⁶Stafford, M. and Hartfield, Jr., R., "Experimental investigation of slot injection into supersonic flow with and adverse pressure gradient," *AIAA Paper 93-2442*, 1993.
- ⁷Lebedev, V., Lemanov, V., Misyura, S., and Terekhov, V., "Effects of flow turbulence on film cooling efficiency," *International Journal of Heat and Mass Transfer*, Vol. 38, No. 11, 1995, pp. 2117–2125.

- ⁸Kanda, T., Ono, F., Takahashi, M., Saito, T., and Wakamatsu, Y., "Experimental studies of supersonic film cooling with shock wave interaction," *AIAA Journal*, Vol. 34, No. 2, 1996, pp. 265–271.
- ⁹Lee, J. and Jung, I., "Effects of bulk flow pulsations on film cooling with compound angle holes," *International Journal of Heat and Mass Transfer*, Vol. 45, 2002, pp. 113–123.
- ¹⁰Richards, B., "Film cooling in hypersonic flow," PhD thesis, University of London, January 1967.
- ¹¹Richards, B. and Stollery, J., "Turbulent gaseous film cooling in hypersonic flow," *The Euromech 21 meeting on Transitional and Turbulent Boundary Layers, Toulouse*, 7th–11th Sep., 1970.
- ¹²Parthasarathy, K. and Zakkay, V., "An experimental investigation of turbulent slot injection at Mach 6," *AIAA Journal*, Vol. 8, No. 7, 1970, pp. 1302–1307.
- ¹³Jr., A. C. and Hefner, J., "Film-cooling effectiveness and skin friction in hypersonic turbulent flow," *AIAA Journal*, Vol. 10, No. 9, 1972, pp. 1188–1193.
- ¹⁴Zakkay, V., Wang, C., and Miyazawa, M., "Effect of adverse pressure gradient on film cooling effectiveness," *AIAA Journal*, Vol. 12, No. 5, 1974, pp. 708–709.
- ¹⁵Richards, B. and Stollery, J., "Laminar film cooling experiments in hypersonic flow," *Journal of Aircraft*, Vol. 16, No. 3, 1979, pp. 177–180.
- ¹⁶Majeski, J. and Weatherford, R., "Development of an empirical correlation for film-cooling effectiveness," *AIAA Paper 88-2624*, 1988.
- ¹⁷Beckwith, I. and Bushnell, D., "Calculation by a finite-difference method of supersonic turbulent boundary layers with tangential slot injection," Tech. rep., NASA TN D-6221, 1971.
- ¹⁸Wang, J., "Prediction of turbulent mixing and film-cooling effectiveness for hypersonic flows," *AIAA Paper 89-1867*, 1989.
- ¹⁹O'Connor, J. and Haji-Sheikh, A., "Numerical study of film cooling in supersonic flow," *AIAA Journal*, Vol. 30, No. 10, 1992, pp. 2426–2433.
- ²⁰Takita, K. and Masuya, G., "Effects of combustion and shock impingement on supersonic film cooling by hydrogen," *AIAA Journal*, Vol. 38, No. 10, 2000, pp. 1899–1906.
- ²¹Lin, Y. and Shih, T., "Film cooling of a cylindrical leading edge with injection through rows of compound-angle holes," *ASME Journal of Heat Transfer*, Vol. 123, 2001, pp. 645–654.
- ²²Badcock, K., Richards, B., and Woodgate, M., "Elements of computational fluid dynamics on block structured grids using implicit solvers," *Progress in Aerospace Sciences*, Vol. 36, No. 5-6, 2000, pp. 351–392.
- ²³Gnoffo, P., "Point-implicit relaxation strategies for viscous, hypersonic flows," *Computational Methods in Hypersonic Aerodynamics*, edited by T.K.S. Murthy, Kluwer Academic Publishers, 1993, pp. 115–151.
- ²⁴Cantariti, F., Dubuc, L., Gribben, B., Woodgate, M., Badcock, K. J., and Richards, B. E., "Approximate Jacobians for the solution of the Euler and Navier-Stokes equations," Technical report, 5, University of Glasgow, UK, 1997.
- ²⁵Wilcox, D., *Turbulence modeling for CFD*, DCW Industries, Inc., 5354 Palm Drive, La Cañada, Calif., 1993.
- ²⁶Menter, F., "Two-equation eddy-viscosity turbulence models for engineering applications," *AIAA Journal*, Vol. 32, No. 8, 1994, pp. 1598–1605.
- ²⁷Yang, X., "Numerical study of film cooling in hypersonic flows," PhD thesis, University of Glasgow, November 2002.
- ²⁸Zeman, O., "Dilatation dissipation: the concept and application in modelling compressible mixing layers," *Physics of Fluids A*, Vol. 2, No. 2, 1990, pp. 178–188.
- ²⁹Seban, R., "Heat transfer and effectiveness for a turbulent boundary layer with tangential fluid injection," *ASME Journal of Heat Transfer, Series C*, Vol. 82, 1960, pp. 303–312.
- ³⁰Goldstein, R., Eckert, E., Tsou, F., and Haji-Sheikh, A., "Film cooling with air and helium injection through a rearward-facing slot into a supersonic air flow," *AIAA Journal*, Vol. 4, No. 6, 1966, pp. 981–985.
- ³¹Hansmann, T., Wilhelmi, H., and Bohn, D., "An experimental investigation of the film-cooling process at high temperatures and velocities," *AIAA Paper 93-5062*, 1993.
- ³²Juhany, K., Hunt, M., and Sivo, J., "Influence of injectant Mach number and temperature on supersonic film cooling," *Journal of Thermophysics and Heat Transfer*, Vol. 8, No. 1, 1994, pp. 59–67.